

[Article ID] 1003- 6326(2002) 05- 0805- 06

## Welding of SiC particle reinforced 6061 Al matrix composite with pulsed TIG<sup>①</sup>

CHEN Mao-ai(陈茂爱), WU Chuansong(武传松), GAO Jin-qiang(高进强)  
(The Key Laboratory of Liquid Structure and Heredity of Materials,  
Ministry of Education, Shandong University, Ji'nan 250061, China)

**[Abstract]** SiC<sub>p</sub>/6061Al alloy composite was welded by using TIG and pulsed TIG welding (P-TIG) without addition of filler metal, or with addition of Al-Si or Al-Mg filler metal. The microstructure and properties of the weld were investigated with XRD, OM, TEM, and MTS-810 testing system was used to observe the effect of different welding procedure and filler metals on the microstructure and properties of the weld. Thermodynamic of SiC-Al reaction was used to analyze the tendency of the reaction between SiC particle and Al matrix during welding. The results showed that the P-TIG tends to produce less plate-like Al<sub>4</sub>C<sub>3</sub> precipitates than TIG; when welding with P-TIG, addition of Al-Si filler metal can not only prevent from formation of Al<sub>4</sub>C<sub>3</sub>, but also decrease hot crack sensitivity of weld; the tensile strength of joint of adding Al-Si filler metal is higher than that of adding Al-Mg filler metal. The SiC<sub>p</sub>/6061Al composite can be successfully welded by P-TIG with addition of Al-Si filler metal.

**[Key words]** SiC<sub>p</sub>/6061Al composite; P-TIG; interfacial reaction; filler metal

**[CLC number]** TG 453.9

**[Document code]** A

### 1 INTRODUCTION

Discontinuously (particle, whisker and short fiber) reinforced aluminum alloy composites have become an attractive structural material for many industrial fields owing to its excellent properties (e. g. high specific strength, high specific stiffness and good wear resistance), low fabrication cost and easiness of secondary processing. They have found application in aviation and automobile industry, for example, automobile drive shaft, brake rotor, connecting rod and piston made from SiC<sub>p</sub>/Al, but their further application is limited by their poor weldability. Therefore special attention has been paid to the joining of this material in recent years. And the solid state joining processes such as friction welding<sup>[1~3]</sup> and diffusion bonding<sup>[4~6]</sup> give encouraging results. However the fusion welding of this material encounters some metallurgical problems. Ahearn et al<sup>[7]</sup> welded SiC<sub>w</sub>/Al with TIG and GMAW and found that the welding exhibited a great number of porosities and delaminations in both weld and HAZ. Devletian<sup>[8]</sup> successfully welded 40% SiC<sub>p</sub>/6061Al, 40% SiC<sub>p</sub>/6061Al to 6061Al with a modified capacitor discharge technique. He also welded 40% SiC<sub>p</sub>/6061Al with TIG, and found that during welding serious reaction between SiC particles and Al matrix occurs and plate-like Al<sub>4</sub>C<sub>3</sub> precipitates form, which are brittle phase and deleterious to the properties of the weld.

The aim of the present work is to seek for possibility of successful welding SiC<sub>p</sub>/6061Al alloy with P-TIG. Both as-received and vacuum-degassed SiC<sub>p</sub>/6061Al are welded. Welding is performed in three

conditions: 1) without addition of filler metal; 2) with addition of Al-Si filler metal; 3) with addition of Al-Mg filler metal. Special attention is given to the microstructure of joint such as particle distribution, reaction products and Al-SiC interface morphology.

### 2 EXPERIMENTAL

#### 2.1 Material

The material used in this investigation was SiC particle reinforced 6061 aluminum composite fabricated by casting method and then rolled to 4.5 mm thick plate. The volume fraction of SiC particle is 10%.

#### 2.2 Welding machine and procedure

The as-received plate of 4.5 mm thick was cut into to be welded pieces of 400 mm in length and 50 mm in width. Before welding, the pieces were cleaned with acetone thoroughly to eliminate dirty and grease. Some pieces were vacuum-degassed prior to welding. The degassing heat treatments were performed at 500 °C for 20 h in a vacuum furnace manufactured by Centorr Industries Inc. Welding experiments were performed with Lincoln Square Wave TIG 355. Single V groove with 90° joint opening was used, leaving 0.5 mm root gap. The compositions of filler metal are listed in Table 1 and the welding parameters in Table 2.

#### 2.3 Microstructure analyses and mechanical testing

① **[Foundation item]** Project (59875053) supported by the National Natural Science Foundation of China

**[Received date]** 2001- 08- 02; **[Accepted date]** 2001- 11- 11

**Table 1** Compositions of filler metal  
(mass fraction, %)

Filler metal	Mg	Mn	Cu	Zn	Si	Ti	Al
AlSi	—	—	≤0.20	≤0.1	4.5~6.0	≤0.20	Bal.
AlMg	5.8~6.8	0.3~0.6	≤0.05	≤0.2	≤0.4	0.02~0.10	Bal.

**Table 2** Welding parameters

$I_p/A$	$I_b/A$	$t_p/(t_p+t_b)$	$f/Hz$	$d_e/mm$	$d_m/mm$
150	50	0.5	4	3.2	2.4

$d_e$ : diameter of tungsten electrode;  $d_m$  diameter of filler metal;  $I_p$ —Peak current;  $I_b$ —Background current;  $t_p$ —Peak time;  $t_b$ —Background time.

Metallurgical specimens were sectioned from the joint along the direction perpendicular to the welding direction. The specimens were first polished with diamond paste and water, and finally polished with diamond paste and alcohol to prevent  $Al_4C_3$  that may be present in the weld from decomposing. After polishing, the specimens were cleaned with acetone. Prepared specimens were analyzed with optical microscopy and X-ray diffraction. X-ray diffraction was performed with a D/max-rc diffractometer on the specimens sectioned from the top of the weld along the welding direction. The AlSiC interface morphology in joint was examined with an H-800 transmission electron microscopy. And the fracture surface was examined with a Philips-515 scanning electron microscopy. The tensile testing was performed on an MTS-810 testing system.

### 3 RESULTS AND DISCUSSION

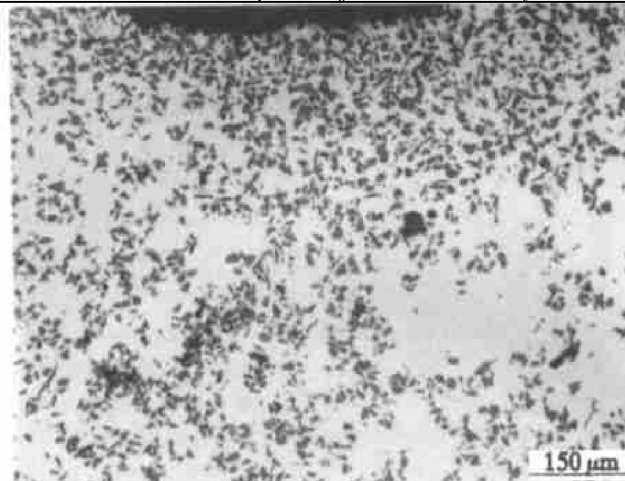
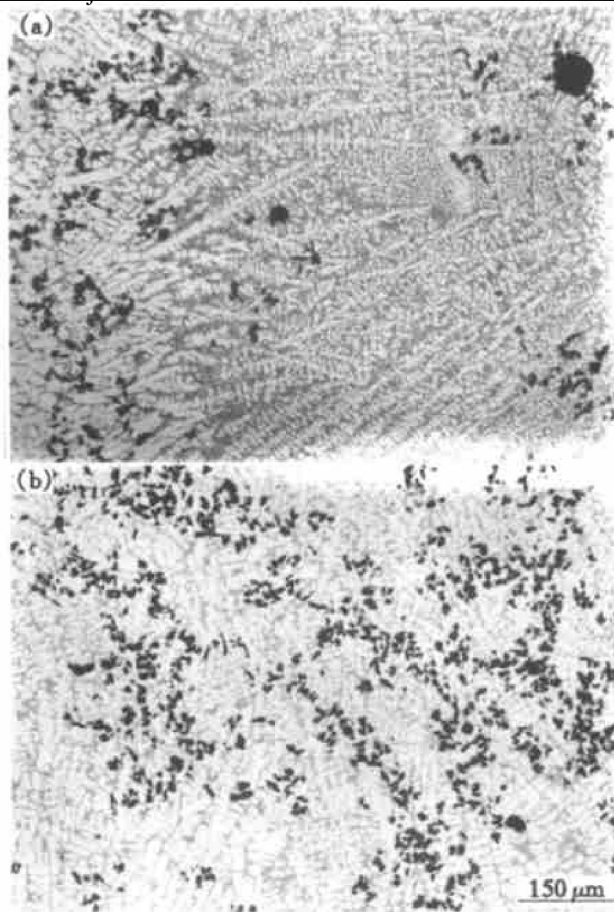
#### 3.1 Particle distribution in joint

When welding without addition of filler metal, the welding pool in SiCp/Al composite was dull and sluggish. This indicates that the viscosity of molten metal is very high and the fluidity is very poor. The surface of the weld pool was dark without metal shine, as though the gas shielding was insufficient. In fact, this was caused by the clustering of SiC particles in the surface of the welding pool. Fig. 1 shows the microstructure of upper part of the P-TIG joint without addition of filler metal, it can be observed that some particles do float up to the surface of the joint and cluster there.

With addition of filler metal, the fluidity of the weld pool was improved greatly and the surface was shiny, indicating that the particle floating-up phenomenon is alleviated and that the joint and filler metal are thoroughly mixed.

Metallographic analyses show that the distribution of particle in weld is not uniform. It can be observed from Figs. 2(a) and 2(b) that there is a zone poor in SiC particles near the fusion line and the dis-

tribution in the center part of joint is relatively uniform.

**Fig. 1** SiC particle distribution in P-TIG joint without addition of filler metal**Fig. 2** SiC particle distribution in P-TIG joint with addition of AlSi filler metal (after vacuum degassed)  
(a) —Area near fusion line;  
(b) —Central area of joint

Such a distribution may be caused by the interaction between the particles and the moving solidification front. During solidification of the welding pool, the particles were rejected by the solidification front. It is considered that solidification rate influences the particle rejection effect of solidification front. As the solid-

ification rate increases, the rejection effect decreases<sup>[9]</sup>. In the area near fusion line, the solidification rate was low, the particles were thus rejected seriously by the solidification front, resulting in a particle-free zone. While in the center of the joint, the solidification rate was relatively high, particle rejection was very weak, as a result, the particle distribution in this area was relatively uniform.

The solidification front pushes the particles, on the other hand, the particles aggregating near the solidification front might influence the solidification of the metal matrix. The particles in the front of the solidification front impeded the diffusion of the solute atom, thus enhancing the constitutional super-cooling. Therefore, the critical solidification rate at which the microstructure changes from equiaxed to columnar might decrease<sup>[10]</sup>. It can be seen from Fig. 2 that columnar grains only occurred in zone near fusion line and frequently interrupted by the particles. Equiaxed grain was susceptible to form in other areas of the joint.

### 3.2 Interfacial reaction

In comparison with P-TIG joints, TIG welds were also produced on the SiC<sub>p</sub>/6061Al composite ( $I = 150$  A, other relevant parameters are the same with P-TIG). The joints were analyzed with X-ray diffraction. Al<sub>4</sub>C<sub>3</sub> diffraction peak was detected in X-ray spectrum of TIG joint without addition of any filler metal, see Fig. 3 (a), and no Al<sub>4</sub>C<sub>3</sub> diffraction peak was detected in P-TIG joint without addition of any filler metal, see Fig. 3 (b). This indicates that the P-TIG welding tends to produce less Al<sub>4</sub>C<sub>3</sub> precipitates than TIG does.

Fig. 4 shows the microstructure of TIG joint without addition of filler metal, Fig. 5 shows the microstructures of P-TIG joint. It can be seen that there are a great number of plate-like precipitates in TIG joint, which were recognized as Al<sub>4</sub>C<sub>3</sub>. While in the P-TIG joint without addition of filler metal and joint with addition of Al-Mg filler metal, only a few Al<sub>4</sub>C<sub>3</sub> precipitates are found, see Fig. 5 (b). In the P-TIG joint with addition of Al-Si filler metal, no Al<sub>4</sub>C<sub>3</sub> precipitate was found; see Fig. 5 (a). This further demonstrates that P-TIG produces less Al<sub>4</sub>C<sub>3</sub> precipitates than TIG does. It can also be concluded that Al-Si filler metal can prevent the formation of Al<sub>4</sub>C<sub>3</sub> precipitate.

The Al-SiC interface morphology in P-TIG joint was examined with the H-800 transmission electron microscopy. The results showed that almost all surface of SiC particles in the joint with addition of Al-Si filler metal is clean and free from any interfacial reaction products, see Fig. 6 (a); while the surface of particles in the joint with addition of Al-Mg filler metal or bead-on-plate weld without addition of filler metal

are much rough and always with plate-like phases existed (Fig. 6 (b)). This phase was clearly identified as Al<sub>4</sub>C<sub>3</sub> by diffraction, see Fig. 3 (a). This further demon-

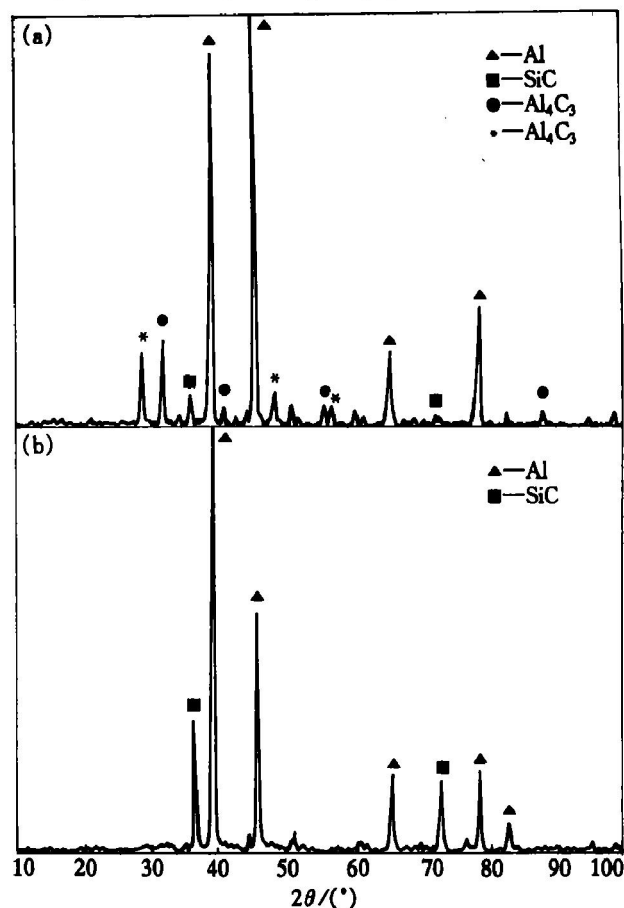


**Fig. 3** X-ray diffraction spectra of weld without addition of filler metal  
(a) —TIG joint; (b) —P-TIG joint

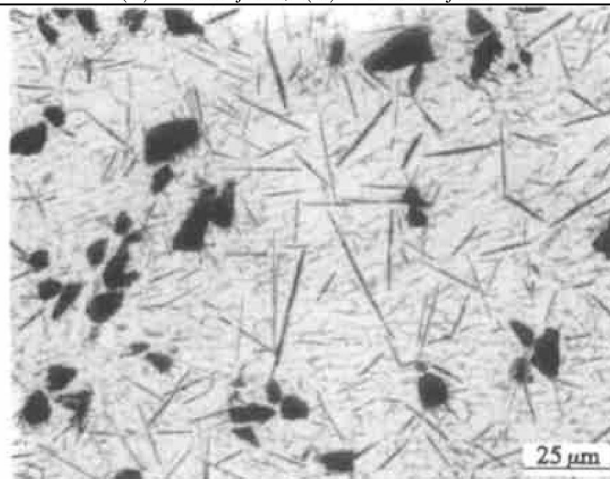


**Fig. 4** Microstructure of TIG joint on SiC<sub>p</sub>/6061 (without addition of filler metal)

strates that Al-Si filler metal can prevent the formation of Al<sub>4</sub>C<sub>3</sub>.

The Al<sub>4</sub>C<sub>3</sub> precipitation was generally considered to form by the following reaction<sup>[11]</sup>:



The interfacial reaction in Al-SiC system<sup>[11]</sup> re-

vealed that the reaction proceeds through three steps: 1) dissolving of SiC in liquid Al and thus generating Si and C; 2) diffusion of C through liquid Al; 3) formation of  $\text{Al}_4\text{C}_3$  near the interface. The rate-limiting step is the dissolving kinetics of SiC in liquid Al and the dissolving rate depends on the surface facet orientation of  $\text{SiC}^{[11]}$ . Therefore the  $\text{Al}_4\text{C}_3$  prefers to form dispersedly near the easy-to-be dissolved part of SiC other than to form a continuous layer around SiC (Fig. 6 (b)).

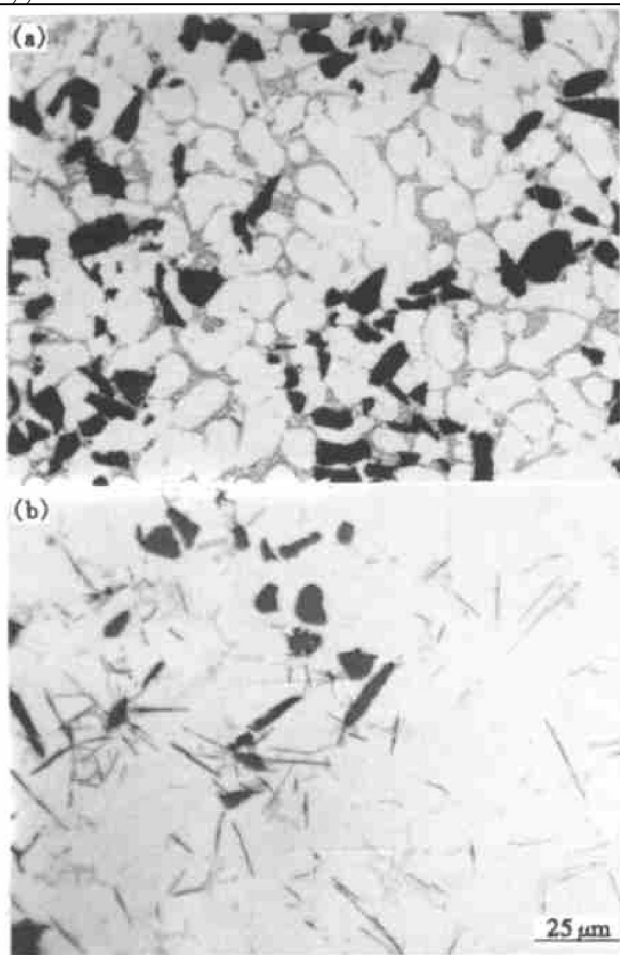


**Fig. 5** Microstructures of P-TIG joint on  $\text{SiC}_p/6061$  (after vacuum degassed)

- (a) —With addition of AlSi filler;  
(b) —With addition of AlMg filler

Iseki et al<sup>[12]</sup> established an expression for standard free energy change  $\Delta G$  as follows:

$$\Delta G = 113\,900 - 12.06T \ln T + 8.92(10^{-3}T^2 + 7.53 \times 10^{-4}T^{-1} + 21.5T + 3RT \ln a_{[\text{Si}]})$$

where  $a_{[\text{Si}]}$  is the activity of Si in liquid Al. It is apparent that the  $\Delta G$  becomes increasingly positive with increasing  $a_{[\text{Si}]}$  and decreasing welding pool temperature.

The temperature of P-TIG welding pool is much lower than that of TIG welding pool, therefore the reaction rate in P-TIG welding pool is much lower. In addition, the rapid welding thermal cycle of P-TIG resulted in a shorter resident time of welding pool, giving less reaction time for the  $\text{SiC}_p/\text{Al}$  interface. Therefore the reaction extent in P-TIG was much lower than that in P-TIG.

The addition of AlSi filler metal would cause the

$a_{[\text{Si}]}$  in the welding pool to increase. The thermodynamic driving force ( $\Delta G$ ) of reaction (1) would thus decrease, and the interface reaction extent would be further reduced or be completely prevented. This is the reason why the P-TIG joint with addition of AlSi filler metal was  $\text{Al}_4\text{C}_3$  free.

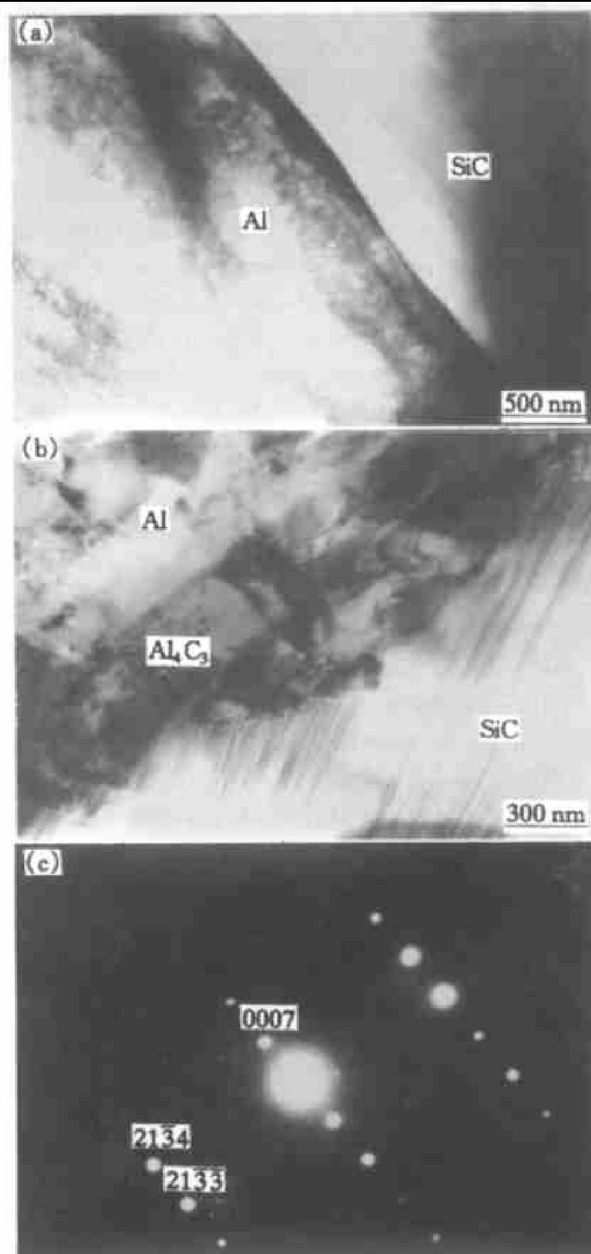


**Fig. 6** TEM images of  $\text{SiC}_p/\text{Al}$  interface in TIG joint

- (a) —With addition of AlSi filler metal;  
(b) —With addition of AlMg filler metal;  
(c) —Diffraction pattern of plate-like phase in (b)

### 3.3 Discontinuities in welding

The joints without prior degassing heat treatment were characterized by large quantity of pores, as shown in Fig. 7. These porosities were generally considered as hydrogen porosities and the hydrogen was released from the matrix metal<sup>[7]</sup>. Increasing the heat input to prolong the resident time of welding pool did not aid in reducing porosities, indicating that hydrogen is difficult to escape from the welding pool during welding. This mainly resulted from the effective



blockage of SiC particle and the poor fluidity of the pool metal. Vacuum degassing heat treatment (degassing at 500 °C, under  $(1.33 \sim 13.3) \times 10^{-3}$  Pa for 20 h) effectively decreased the porosities, see Figs. 2 and 5, suggesting that the high porosity susceptibility of SiC<sub>p</sub>/Al weld is also attributed to the high content of hydrogen in the SiC<sub>p</sub>/Al composite. Therefore it is imperative that prior degassing heat treatment be performed.

Longitudinal hot-crack of 10 mm long was always found on every joint with addition of AlMg filler metal or bead-on-plate joint without addition of any filler metal, while no macro-crack was observed on the joints with addition of AlSi filler metal. This indicates that the addition of AlSi filler metal will reduce the hot-crack sensitivity. This is mainly because that the AlSi eutectic improves the fluidity of the molten metal. A few short micro-cracks were found in the arc-extinguishing end of the weld with addition of AlSi filler metal, as shown in Fig. 8. It was obvious that the hot-crack susceptibility of SiC<sub>p</sub>/6061Al was higher than that of 6061 Al alloy. The possible reasons were: 1) fluidity of molten metal during the last stage of solidification was much lower because

of low fluidity due to the clustering of SiC particle<sup>[8]</sup>; 2) the expansion coefficient difference between the parent composite and the welding metal exaggerated the tensile stress in the welding joint.

### 3.4 Mechanical properties and fracture analyses

Only the mechanical properties of P-TIG joints were measured, because most of TIG joint ruptured during the fabrication of test pieces. Test pieces were cut from the central part of P-TIG joint in the transverse direction, with their transversal central lines aligned with the longitudinal central lines of joints. Before testing, the reinforcements were removed. The tensile testing results were summarized in Table 3. All the test pieces failed in the welding metal, indicating that the strength of joint is controlled by that of the welding metal. The joint without prior degassing heat treatment exhibited lower tensile strength and elongation due to the higher porosity density and size. The joint with addition of AlMg filler metal exhibited lower tensile strength and elongation than the joint with addition of AlSi filler metal did because of the interfacial reaction between Al and SiC.

**Table 3** Tensile properties of P-TIG welds on SiC<sub>p</sub>/6061Al

Specimen	Treatment prior to welding	Condition of welding	Tensile strength / MPa	δ / %
Parent material	T6	—	303	5.6
			210	4.1
Welding with addition of AlSi filler metal	Vacuum degassed	As welded	201	4.4
			218	4.9
			131	1.3
	Undegassed	As welded	110	1.5
			97	1.4
			165	2.4
Welding with addition of AlMg filler metal	Vacuum degassed	As welded	153	2.3
			169	1.8
			122	1.2
	Undegassed	As welded	108	1.4
			101	1.0

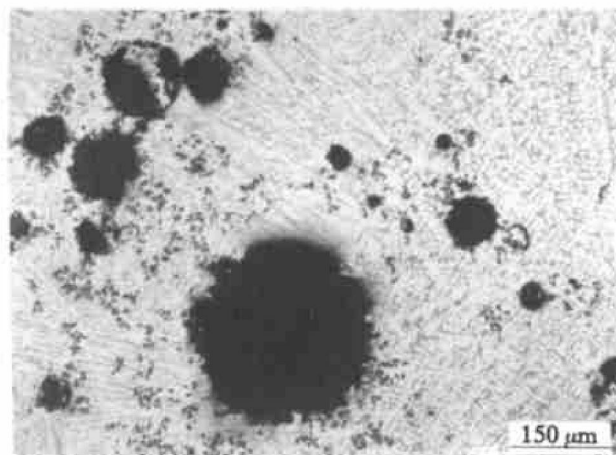


**Fig. 7** Porosity in P-TIG joint on SiC<sub>p</sub>/6061Al (undegassed)

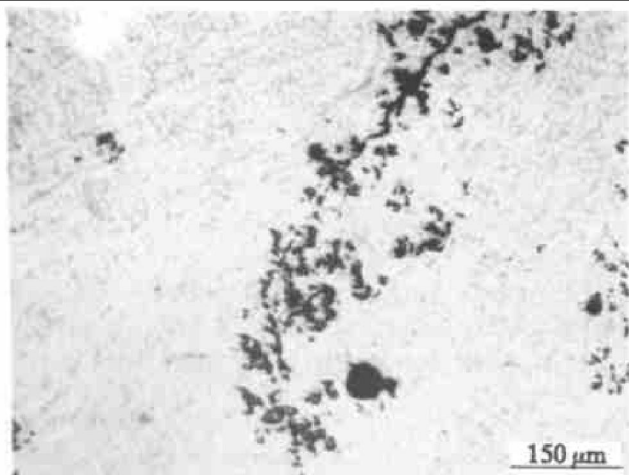


**Fig. 8** Microcrack in P-TIG joint with addition of AlSi filler metal

Fig. 9 shows the typical fracture morphologies of different P-TIG joints. The fracture surface of joint without prior degassing heat treatment exhibited many porosities, see Fig. 9(a). The fracture surface of joint with addition of AlSi filler metal exhibited more ductile dimples than that of joint with addition of AlMg filler metal, as shown in Figs. 9(b) and (c).

From these observations, it is apparent that the porosities and interfacial reaction are responsible for the low tensile strength and elongation. Lloyd also found that both voids and failure of interface play an

important part in the failure of SiC<sub>p</sub>/Al composite<sup>[9]</sup>. It is well accepted that the porosities are susceptible to initiate crack, thus resulting in a much lower tensile strength. And the Al<sub>4</sub>C<sub>3</sub> crystals behave just like voids because of their brittleness, they are also susceptible to initiate cracks<sup>[12]</sup>.

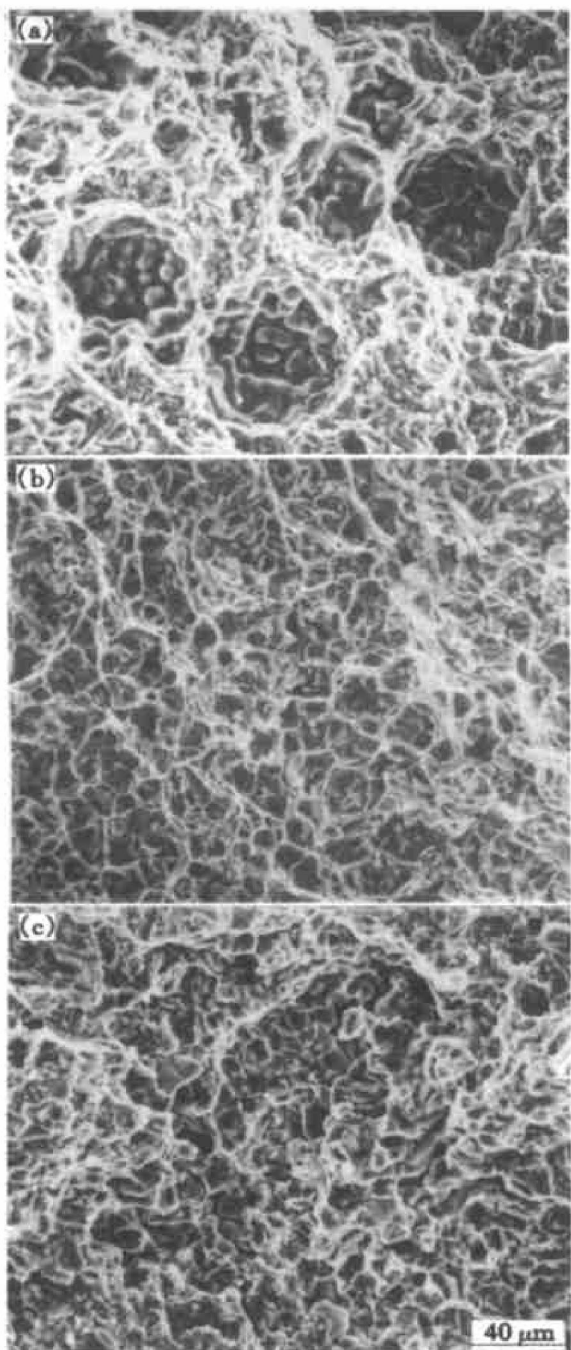


**Fig. 9** SEM fractographs of P-TIG joint on SiC<sub>p</sub>/6061Al

(a) —With addition of AlSi filler metal, undegassed; (b) —With addition of AlSi filler metal, degassed; (c) —With addition of AlMg filler metal, degassed

#### 4 CONCLUSIONS

1) SiC<sub>p</sub>/6061Al is successfully welded with P-TIG welding with little or no Al<sub>4</sub>C<sub>3</sub> formed, while

the TIG tends to produce a large number of plate-like Al<sub>4</sub>C<sub>3</sub> precipitates.

2) With addition of filler metal, the matrix metal and filler metal are completely mixed, but the particle distribution is not uniform, and there is a zone poor in particle near the fusion line, this may be attributed to the rejection effect of solidification front.

3) SiC<sub>p</sub>/6061Al welding joint exhibits high porosity susceptibility and hot-crack susceptibility.

4) Addition of AlSi filler metal can not only prevent from formation of Al<sub>4</sub>C<sub>3</sub>, but also reduce the hot crack sensitivity of the welding joint. Therefore the joint with addition of AlSi filler metal exhibits higher strength and elongation than that with addition of AlMg filler metal.

#### [ REFERENCES ]

- [ 1 ] Midling O T, Grong Φ. A process model for friction welding of AlSiMg alloys and AlSiC metal matrix composites—Part I: HAZ temperature and strain rate distribution [ J ]. *Acta Metal Mater*, 1994, 42(5): 1595– 1600.
- [ 2 ] Midling O T, Grong Φ. A process model for friction welding of AlSiMg alloys and AlSiC metal matrix composites—Part II: HAZ microstructure and strength evolution [ J ]. *Acta Metal Mater*, 1994, 42(5): 1611– 1623.
- [ 3 ] Kazuyoshi K, Hiroshi T. Weld interface of friction welded joints of Al alloy composite to Al alloys [ J ]. *Welding of Light Metal*, 1994, 32(10): 429– 433.
- [ 4 ] Partridge P G, Sheperd M, Dunford D V. The role of interlayers in diffusion bonded joints in metal matrix composites [ J ]. *J Mater Sci*, 1991, 26(12): 2255– 2262.
- [ 5 ] Zhan Y P, Ye L, Mai Y W. Investigation on diffusion bonding characteristic of SiC particle reinforced Al metal matrix composites [ J ]. *Composites*, 1999, 30(10): 1415– 1421.
- [ 6 ] Urena A, Gomez de Salazar J M, Escalera M D. Diffusion bonding of discontinuously reinforced SiC/Al matrix composite: the role of interlayers [ J ]. *Key Engineering Materials*, 1995, 104– 107: 523– 540.
- [ 7 ] Ahearn J S, Cooke C, Fishman S G. Fusion welding of SiC-reinforced Al composite [ J ]. *Metal Construction*, 1982, 14(4): 192– 197.
- [ 8 ] Devletian J H. SiC/Al metal matrix composite welding by a capacitor discharge process [ J ]. *Welding Journal*, 1987, 66(6): 33– 39.
- [ 9 ] Lloyd D J, Lagace H, Mcleod A, et al. Microstructure aspects of aluminum-silicon carbide particulate composite produced by a casting method [ J ]. *Mater Sci Eng*, 1989, A107(1): 73– 80.
- [ 10 ] XIE Guo-hong. Solidification mechanisms of SiC reinforced aluminum composite, (in Chinese) [ D ]. Shanghai: Shanghai Jiaotong University, 1995: 45– 48.
- [ 11 ] Handwerker A C, Ursula M D, Kattner R. Interface reactions and phase stability in the AlSiC system [ A ]. *Advance in Joining Newer Structure Materials* [ C ]. London: Pergamon Press, 1990: 129– 137.
- [ 12 ] Iski T, Kameda T, Maruyama T, et al. Interfacial reactions between SiC and Al during joining [ J ]. *J Mater Sci*, 1984, 19(10): 1692– 1698.

( Edited by HUANG Jin-song )